Selective reactivation of value- and place-dependent information during sharp-wave ripples in the intermediate and dorsal hippocampus

Seung-Woo Jin and Inah Lee*

Department of Brain and Cognitive Sciences
Seoul National University
Gwanak-ro 1, Gwanak-gu
Seoul, Korea
08826

*Corresponding author:
E-mail: inahlee@snu.ac.kr
Phone: +82-2-880-8013

Abbreviated title: Value-dependent reactivation in the hippocampus

Keywords: dorsal hippocampus, intermediate hippocampus, place cell, sharp-wave ripple, reactivation

Summary

Reactivation of place cells during sharp-wave ripples (SWRs) in the hippocampus transfers newly acquired information to the neocortex and thus is important for memory consolidation. However, whether hippocampal reactivation is affected by the values of events experienced by the animal is largely unknown. Here, we investigated whether place cells in the dorsal (dHP) and intermediate (iHP) hippocampus are differentially reactivated depending on the value associated with a place. Rats were trained to learn the places associated with higher-value rewards in a T-maze, with concurrent simultaneous recording of single units in the dHP and iHP. Place cells in the iHP representing the high-value location were reactivated significantly more frequently during SWRs in both task and subsequent sleep periods than those representing the low-value location. The amount of reactivation during sleep was positively correlated with learning speed the next day. In contrast, these characteristics were not observed in the dHP. Instead, place-cell activities coding the routes leading to high-value locations were replayed more in the dHP than in the iHP. Our findings suggest that value-based differential reactivation patterns along the septotemporal axis of the hippocampus may play essential roles in goal-directed spatial-learning optimization for maximal reward.

Introduction

The hippocampus plays a critical role in episodic memory (Eichenbaum 2000, Eichenbaum and Cohen 2001, Squire et al. 2004), which often consists of events associated with different values occurring in space. In the hippocampus, highly synchronized activities of place cells are entrained during sharp-wave ripples (SWRs), and the firing sequences during recent wakeful experiences are re-expressed during SWRs (Wilson and McNaughton 1994). These findings have given rise to the hypothesis that reactivation of place cells contributes to the consolidation process by transferring the newly obtained hippocampal information to neocortical networks (Buzsaki 1989).

It is important to note that prior studies focused mostly on investigating the sequential firing patterns of place cells in the dorsal hippocampus (dHP). For example, it has been demonstrated that an animal's recent navigational traces or upcoming paths leading to a goal location are reactivated ("replayed") in the dHP during SWRs (Foster and Wilson 2006, Pfeiffer and Foster 2013). What is largely unknown is whether such reactivations are modulated by different values associated with places. Also, if such value-dependent differential reactivation does occur in the hippocampus, does it occur differentially across different subregions along the longitudinal axis of the hippocampus? A previous study reported that SWRs and replay events occur more frequently in the dHP when a larger reward is provided (Ambrose et al. 2016). Another study showed that the routes associated with larger rewards are replayed more in the dHP than those with smaller rewards (Michon et al. 2019). However, whether such value-based modulation of replay also occurs in other hippocampal regions is still largely unknown.

In our previous study, we found that the place fields of place cells in the iHP were immediately remapped in response to a change in value at a reward location in the T-maze, coalescing around the location associated with the higher-value reward rather than the lower-value reward (Jin and Lee 2021). Other researchers have reported that a subset of place cells in the iHP are dedicated to coding reward information through remapping of their fields to a new place where a reward is available (Gauthier and Tank 2018, Jarzebowski et al. 2022). Therefore, the place cells activated in the dHP and iHP during a navigation task in which places are differentiated by different reward values may also be reactivated differentially during SWRs. We hypothesize that, in the iHP, the neural activities of place cells representing higher-value locations are reactivated more than those

representing lower-reward locations, and that such neural firing characteristics may not occur in the dHP, as suggested by our prior study (Jin and Lee 2021),.

To test the above hypothesis, we simultaneously recorded neural activities from single units in the dHP and iHP while rats performed a place-preference task on a T-maze (Jin and Lee 2021). We found that place cells in the iHP representing higher-value locations were reactivated more frequently than those coding lower-value locations. However, this value-dependent reactivation pattern was not observed in the dHP. Instead, precise spatial trajectories that sequentially lead to the goal locations were replayed in the dHP, whereas no sequential replay was observed in the iHP. This double dissociation between the iHP and dHP suggests that functionally heterogeneous information content is reactivated during SWRs in different hippocampal regions when goal-directed navigation requires differentiating places based on their values.

Results

Behavioral performance in the place-preference task

Rats were trained in a place-preference task on a T-maze (Figure 1A; Video S1). Briefly, in Block 1, rats were required to find the high-value reward arm (HiV-arm) against the low-value reward arm (LoV-arm) by trial and error until they reached the learning criterion (Figure 1A). To encourage hippocampal-based learning and discourage eliciting a response strategy (Packard and McGaugh 1996), in Block 2, rats were started from the opposite side of the original starting point used in Block 1. The spatial relationships between the arms and their reward values were then reversed in Block 3, requiring rats to update the place and its value information (Figure 1A). Spiking activities were recorded from single units in the hippocampus while rats performed the task. Single-unit recordings were also obtained when rats were asleep or immobile before and after the place-preference task (approximately 30 minutes per sleep session).

Reward values were manipulated both qualitatively and quantitatively. Specifically, in sessions 1 and 2 (i.e., *qualitative value-differentiation session*, or *Qlt-VD*), a quarter of a sunflower seed and a quarter of a Cheerios were used as high- and low-value rewards, respectively (Figure 1B). In sessions 3 and 4 (i.e., *quantitative value-differentiation session*, or *Qnt-VD*), a whole sunflower

seed and a quarter of a sunflower seed were used as high- and low-value rewards, respectively (Figure 1C). To estimate the trial in which the rat learned the HiV-arm (*acquisition onset*) in each block, we applied a state-space model to behavioral performance data (Smith et al. 2004). Compared to Blocks 1 and 2, learning took place slower in Block 3 ($p < 0.001$ for both Block 1 and 2 vs. 3 in Figure 1D; Wilcoxon signed-rank test with Bonferroni corrections) (Figure 1D). This difference reflected the fact that rats continually visited the LoV-arm because that arm had been baited with high-value rewards in previous blocks. The delayed onset of acquisition in Block 3 compared to Block 2 cannot be ascribed to a decrease in motivation because their latencies were similar between Blocks 2 and 3 ($p > 0.1$ for Block 2 vs. 3 in Figure 1E; Wilcoxon signed-rank test). Because the shape of the estimated learning curve and the timing (i.e., trial) of acquisition onset were similar between Qlt-VD and Qnt-VD, neural signals recorded from the two types of sessions were pooled in subsequent analyses.

Frequent occurrence of SWRs in the reward zone and during the inter-trial interval period

Single-unit spiking activities and local field potentials (LFPs) were simultaneously recorded from the dHP and iHP, defined as in our previous study (Jin and Lee, 2021), while rats performed the place-preference task. The SWRs (150-250 Hz) used for analysis were recorded from CA1 pyramidal cell layers in the dHP and iHP (Figure S1A and S1B). SWRs were characterized by large amplitudes (>4 standard deviations [SDs]) and coactivation of at least 5% of cells recorded in a given session while rats showed minimal movement (Figure 2A and 2B; Figure S2A and S2B; see Methods for details). Putative inhibitory interneurons were excluded from subsequent analyses (Figure S1C). Most putative complex spike cells were recorded from the CA1 (Figure S1D).

Based on our SWR-detection criteria, most SWR events (80-85%) occurred while rats were located in reward zones consuming the reward or during inter-trial interval (ITI) periods while rats waited for the next trial (Figure 2C and 2D; Figure S2A and S2B). Similar proportions of SWRs occurred between the reward zone and ITI period in the dHP (Figure 2D). However, approximately half of SWR events in the iHP occurred while rats were in the reward zone, suggesting that the effect of the reward on the occurrence of SWRs was greater in the iHP than in the dHP ($p < 0.001$ for group comparison; $p < 0.001$ for reward zone and ITI conditions; Chi-square test with Bonferroni corrections) (Figure 2D). To better align with the hypothesis of the current study, which focuses on reward value-related reactivation in the dHP and iHP, we restrict our analysis of SWR events to the

reward zones, reflecting the high likelihood of a substantial disparity in the proportion of SWR events within these zones between the dHP and iHP.

Reactivation of place cells representing high-value locations during SWRs in the iHP but not in the dHP

To test whether place cells encoding high-value or low-value arms are differentially reactivated during SWRs, we analyzed place cells whose place fields were located on either the HiV-arm or LoV-arm in the T-maze. The extent to which spatial firing patterns changed upon reversal of reward contingency was measured by determining Pearson's correlation coefficients between rate maps before and after reward reversal. If the correlation coefficient was greater than 0.75, place cells recorded in the HiV-arm were classified as non-remapping place cells (NRM_{Hi}); otherwise, they were classified as remapping place cells (RM_{Hi}) (Figure 3A and 3B). The same criterion was applied to place cells recorded in the LoV-arm (NRM_{Lo} and RM_{Lo}). Because rate maps for non-remapping place cells (NRM_{Hi} and NRM_{Lo}) showed high similarities before and after the reversal manipulation, these cells are considered to primarily represent location information (i.e., location-coding place cell). In contrast, remapping cells (RM_{Hi} and RM_{Lo}) underwent significant global remapping after the reward reversal, suggesting that these cells are significantly modulated by the reward value associated with the arms (i.e., spatial-value-coding place cell). The numbers of cells representing HiV-arm and LoV-arm were similar to each other in the iHP ($n = 72$ for RM_{Hi} and NRM_{Hi}, $n = 75$ for RM_{Lo} and NRM_{Lo}; $p > 0.1$ for one-sample Chi-square test) and in the dHP ($n = 55$ for RM_{Hi} and NRM_{Hi}, $n = 63$ for RM_{Lo} and NRM_{Lo}; $p > 0.1$; one-sample Chi-square test), suggesting that location- and spatial-value–coding place cells are uniformly distributed in HiV- and LoV-arms (Figure 3C).

Since location- and spatial-value-coding place cells were best dissociated in Block 3, in which rats learned the reversal task, SWR-based reactivation patterns were further analyzed only in the reversal block. Specifically, we examined if place cells representing the high-value arm (RM_{Hi}) were reactivated more frequently than those representing the low-value arm (RM_{Lo}) or location-coding place cells (NRM_{Hi} and NRM_{Lo}). Individual SWR examples showed that, among the four cell types (NRM_{Hi}, RM_{Hi}, NRM_{Lo}, and RM_{Lo}), spiking activities of RM_{Hi} cells were reactivated exclusively during SWRs in the reversal block (i.e., Block 3) in the iHP (Figure 4A). We measured the probability of co-reactivation of RM_{Hi} cells with other types of cells in the iHP, and found that RM_{Hi} cells in the iHP were more likely to fire together only with the same cell type (RM_{Hi}) during

SWRs, and not with other cell types (NRM_{Hi}, NRM_{Lo}, and RM_{Lo}) ($p < 0.001$; Kruskal-Wallis test) (Figure 4B). Furthermore, a single RM_{Hi} cell in the iHP had a significantly higher probability of reactivation during SWRs than other cell types ($p < 0.01$ for RM_{Hi} vs. NRM_{Hi}, $p < 0.05$ for RM_{Hi} vs. RM_{Lo} and NRM_{Lo}; Wilcoxon rank-sum test with Bonferroni corrections) (Figure 4C).

In contrast, in the dHP, all cell types tended to be reactivated equally during SWRs (Figure 5A). This is further supported by the probability of co-reactivation of RM_{Hi} cells with other cell types ($p > 0.1$; Kruskal-Wallis test) (Figure 5B). In addition, individual RM_{Hi} cells in the dHP had similar probabilities of reactivation during SWRs compared with other types of cells ($p > 0.1$ for RM_{Hi} vs. NRM_{Hi}, NRM_{Lo}, and. RM_{Lo}; Wilcoxon rank-sum test with Bonferroni corrections) (Figure 5C). This difference between the dHP and iHP was also confirmed by a comparison of reactivation rates (Figure S3A). The higher reactivation probabilities of RM_{Hi} cells in the iHP cannot be attributed to the higher excitability of this cell type because the peak firing rates of individual place cells and their reactivation probabilities were not significantly correlated (Figure S3B). Our findings thus suggest that the exclusive reactivation of place cells representing high-value locations during SWRs is a unique property of the iHP.

Exclusive potentiation of the reactivation of place cells representing the high-value location upon learning

We next investigated whether reactivation of RM_{Hi} cells during SWRs in the iHP was modulated by reward value and learning state. First, we divided trials in the pre-learning state into correct and incorrect. Only correct trials were used in the post-learning state because very few incorrect trials (thus very few SWRs) were found after rats acquired the task (Figure S2C). Examples of individual ripples showed that, before learning, reactivation of RM_{Hi} cells in the iHP was not noticeable in correct and incorrect trial types (Figure 6A). However, after rats learned the task (i.e., acquisition onset), RM_{Hi} cells in the iHP started to fire exclusively during SWRs, while other cell types remained silent. These results suggest that the exclusive reactivation of RM_{Hi} cells in SWRs in the iHP is learning-dependent. In contrast, in the dHP, four cell types were reactivated with similar proportions regardless of the learning state or trial type (Figure 6B).

At the population level, the reactivation probabilities of RM_{Hi} cells in the iHP increased significantly in correct trials of the post-learning state compared to that in the pre-learning state (Figure 6C) ($p < 0.05$ for post-learning and correct trials vs. pre-learning and correct trials; $p < 0.001$

for post-learning and correct trials vs. pre-learning and incorrect trials; Wilcoxon rank-sum test). Such learning-dependent changes were not observed in RM_{Hi} cells in the dHP (Figure 6D) ($p > 0.1$ for all comparisons; Wilcoxon rank-sum test). Unlike RM_{Hi} cells, RM_{Lo} cells in the iHP showed no significant increase in the probability of SWR-based reactivation after learning compared to the pre-learning state, although there was a slight, yet significant, increase in incorrect trials during the pre-learning state (Figure S4A). Similar results were obtained using the reactivation rate as an alternative measurement (Figure S4B and 4C). However, we did not find significant learning-dependent changes in reactivation patterns in the dHP (Figure 6D; Figure S4D and S4F). Collectively, these results suggest that reactivation of place cells representing the high-value location upon reversal in the iHP may play a critical role in consolidating the newly learned spatial value.

Selective reactivation of high-value-location–representing place cells in the iHP during the sleep period after learning is correlated with the next day's place-value learning

To determine whether the potentiated reactivation of RM_{Hi} cells in the iHP persists in the post-sleep period following a behavioral recording session, we examined reactivation patterns during pre- and post-sleep sessions using the same place cells shown in Figure 4. RM_{Hi} cells in the iHP were not reactivated during SWRs in the pre-sleep period (Figure 7A). However, after the rat experienced the place-preference task, reactivation of this cell type was observed exclusively in the post-sleep period. In contrast, there was no detectable change between pre- and post-sleep periods in the dHP (Figure 7B).

Measurements of relative changes in the probability of co-reactivation between pre- and post-sleep periods revealed a significant increase in the co-reactivation probability of the RM_{Hi} cell type in the iHP in the post-sleep period compared to the pre-sleep period ($p < 0.01$; Kruskal-Wallis test) (Figure 7C). Also, the relative increase of reactivation probability in post-sleep compared to pre-sleep period was significantly higher in the RM_{Hi} cells than other cell types in the iHP ($p < 0.01$ for RM_{Hi} vs. NRM_{Hi} and vs. RM_{Lo}, $p < 0.05$ for RM_{Hi} vs. NRM_{Lo}; Wilcoxon rank-sum test with Bonferroni corrections) (Figure 7D). In contrast, such significant changes between sleep sessions were rarely observed in the dHP (Figure 7C and 7D). Separate analyses of the reactivation activities of pre- and post-sleep sessions confirmed these findings (Figure S5).

Importantly, we found that RM_{Hi} cells that exhibited higher reactivation probabilities during SWRs in the behavioral session also showed higher reactivation probabilities in the post-sleep period

than pre-sleep period ($p < 0.05$, $r^2 = 0.20$; linear regression) (Figure 7E). Furthermore, the increase in reactivation probabilities of RM_{Hi} cells in the iHP during post-sleep compared to pre-sleep was positively correlated with the learning speed in Block 1 on the next day (i.e., the inverse of acquisition onset) ($p < 0.05$, $r^2 = 0.56$; linear regression) (Figure 7F). No such positive correlations were found for other cell types in the iHP (Figure S6) or between reactivation and learning speed in the dHP (Figure 7G and 7H). Our findings suggest that reactivation of RM_{Hi} cells in the iHP during sleep may underlie the consolidation of value-updated location information.

Sequential spatial reactivation of place cells that lead to the high-value reward location is found only in the dHP

Finally, we tested if sequential reactivation (i.e., spatial replay) of place cells occurred in our task in both the dHP and iHP, as previously reported (Foster and Wilson 2006). We calculated the posterior probability using Bayesian decoding for place cells recorded simultaneously during a SWR event (Figure 8A and 8B). In the dHP, we observed robust reverse replay (ripples #1-4 in Figure 8C) or forward replay (ripples #5-8 in Figure 8C) within individual SWR events. However, no such robust spatial replays were observed in the iHP. Instead, place cells in the iHP seemed to collectively reactivate spatial representations near either the intersection of the T-maze (ripples #1-4 in Figure 8D) or the choice arms (ripple #5-8 in Figure 8D).

The proportion of spatially replayed place fields in the dHP was significantly higher than that in the iHP ($p = 0.0019$; two-sample Chi-square test) (Figure 8E). More importantly, 65% of spatial replay occurred during high-value trials, and most of the replay represented the rat's navigational paths leading to the high-value reward zone. Although 35% of replay occurred in low-value trials, sequential reactivation of routes leading to the high-value reward zone was observed more frequently than those leading to low-value zones in those trials ($p = 0.058$; one-sample Chi-square test) (Figure 8F). The robust spatial replay observed in the dHP also suggests that the lack of reward value-related changes in the reactivation patterns of place cells in the dHP compared to the iHP cannot be attributed to idiosyncratic experimental conditions of the current study.

Discussion

The current study investigated whether place cells in the iHP are reactivated differentially during SWR events after learning spatial value changes. We found that place cells representing high-value locations (RM_{Hi}) in the iHP were reactivated more frequently after spatial value reversal than low-value-location–coding place cells (RM_{Lo}) or location-coding place cells (NRM_{Hi} and NRM_{Lo}). Furthermore, selective reactivation of RM_{Hi} cells in the iHP was enhanced after rats learned the task after spatial value reversal; moreover, this potentiated reactivation of RM_{Hi} cells in the iHP was maintained in the post-sleep period. Importantly, the frequent reactivation of RM_{Hi} in the iHP during the post-sleep period facilitated place-value learning the next day. However, such value-based, learning-dependent reactivation was rarely observed in the dHP. Instead, we found that the spiking activities of place cells whose place fields were sequentially organized toward the high-value reward location were replayed more frequently in the dHP than in the iHP during SWRs. Overall, our findings suggest that functionally heterogeneous types of information are differentially and simultaneously reactivated in the dHP and iHP to facilitate goal-directed navigation-optimization for maximal reward.

Spiking activities representing high-value locations are selectively reactivated in the iHP but not in the dHP

In our experiments, we assumed that a subset of place cells that remapped their fields to represent high-value locations (RM_{Hi}) are specialized to encode the high value of a place. We found that RM_{Hi} cells in the iHP had higher reactivation probabilities than RM_{Lo} cells or location-coding place cells. These results suggest that the relative value of information associated with a place can modulate the reactivation probabilities of place cells in the iHP. Although some prior studies have suggested that the function of the iHP is to encode and update the value of a place, to the best of our knowledge, the type or quality of information reactivated in the iHP has rarely been previously reported (Bast et al. 2009, De Saint Blanquat et al. 2013, Jin and Lee 2021).

In our previous study (Jin and Lee 2021), we found that place cells in the iHP exhibited more robust remapping in response to changes in reward value than those in the dHP, and their fields accumulated near high-value locations. Another study by De Saint Blanquat et al. (2013) showed

that inactivating the iHP by injection of muscimol impaired place-value updating in place-preference tasks, but no impairment was observed when the dHP was similarly inactivated. Furthermore, lesioning the iHP impaired the rapid learning of a place-learning task in which the location of the hidden escape platform changed daily (Bast et al. 2009) and abolished the goal-related activities of the medial prefrontal cortex in the place-preference task (Burton et al. 2009). These results imply that high-value–associated spatial information is reactivated selectively in the iHP and serves to facilitate associative learning between a place and its value.

In contrast, we found no such reactivation patterns in the dHP. Most studies of the dHP have focused on reinstatement of navigational trajectories (spatial replay) by sequential spatial firing (Widloski and Foster 2022, Mou et al. 2022, Igata et al. 2021, Gillespie et al. 2021, Bhattarai et al. 2020). However, few studies have directly investigated whether the reactivation patterns of cells are dependent on the relative values associated with different places in the dHP. It is worth noting that some study results imply that reward information can modulate the reactivation probabilities of place cells in the dHP. For example, Ambrose et al. (2016) showed that the frequency of reverse replay in the dHP was manipulated by the amount of reward provided in the reward zone in an experimental paradigm in which rats shuttled between two reward zones in a linear maze. Another study by Singer and Frank (2009) argued that reactivation responses were enhanced in the reward compared to the no-reward condition. These results are seemingly in conflict with other studies demonstrating that place cells in the dHP tend to exhibit value-insensitive firing when values associated with fixed reward locations changed (Jin and Lee 2021, Duvelle et al. 2019, Tabuchi et al. 2003). This discrepancy may reflect the difference in behavioral tasks; in this case, rats were required to update spatial value from a low-value (i.e., a small amount of reward) to a high-value (i.e., a large amount of reward) in a goal-directed navigational task (Jin and Lee 2021, Duvelle et al. 2019, Tabuchi et al. 2003). In contrast, other studies used non-hippocampal shuttling tasks (Ambrose et al. 2016) or provided rewards only in one of two reward zones in a W-shaped maze (Singer and Frank 2009).

Notably, some prior studies manipulated spatial value by associating an electric shock with a place (Moita et al. 2004). In this scenario, place fields in the dHP underwent global remapping after the animal experienced the electric shock. Our results are consistent with the idea that the spiking activities of place cells that remapped after associating a negative value with a certain place could also be reactivated more frequently than non-remapping cells. Ormond et al. (2023) tested this idea using an aversive spatial decision-making task in which rats received an electric shock in the choice

arm. After experiencing the shock, rats did not re-enter the shock-associated arm, and a subset of place cells in the dHP remapped their fields globally. Importantly, reactivation probabilities were higher in place cells that exhibited shock-related remapping in the dHP than in non-remapping cells. In another study, rats received an electric shock at the end of a linear track (Wu et al. 2017). After the shock experience, rats avoided the shock zone as they moved around on the track, and the place cells whose fields were located in the shock zone in the pre-shock trials were reactivated more frequently during SWRs than those representing the non-shock zone in the pre-shock period. These results suggest that a negative event at a particular location changes the value of the place and may alter the probability of reactivation of the cells representing the location, serving to strengthen the associative memory between the place and its value during SWRs.

Sequential spatial representations leading to the high-value location are replayed in the dHP but not in the iHP

Previous studies reported that spatial paths leading to goal locations are sequentially replayed more in the dHP than those leading to non-goal locations (Pfeiffer and Foster 2013, Michon et al. 2019, Igata et al. 2021). Based on our prior study that place cells in the iHP overrepresent high-value locations compared with low-value locations (Jin and Lee 2021), we originally expected spatial replays leading to goal locations to occur more frequently in the iHP than the dHP. However, sequential reactivation of spatial representations leading to high- and low-value locations was barely detectable in the iHP. Instead, we found robust spatial replays in the dHP, as has been frequently reported (Foster and Wilson 2006, Karlsson and Frank 2009, Diba and Buzsaki 2007). The iHP may not be an ideal region for the occurrence of such sequential replays of precise location information because the size of the place field is larger and spatial tuning is poorer in the iHP compared with the dHP (Jin and Lee 2021, Kjelstrup et al. 2008, Jung et al. 1994). Instead, the larger place fields in the iHP may make the area suitable for representing spatial values, given that the spatial resolution of value is expected to be lower than that of a place in a natural environment.

In the current study, 85% of replay events in the dHP represented sequential paths to the higher-value location, whereas only 15% of replay events represented paths to the low-value location. Thus, the direction of spatial replay in the dHP seems biased toward the high-value

location, which aligns with prior studies well (Pfeiffer and Foster 2013, Michon et al. 2019, Igata et al. 2021). For example, using a dual-environment reward-place association task on an eight-arm maze, Michon et al. (2019) found that hippocampal replay events are biased toward paths associated with high-value (i.e., large reward) locations compared with those associated with low-value reward locations. Other studies reported that, when rats learned the location associated with reward in an open arena, trajectories leading to that location were replayed more frequently than those leading to no-reward locations (Pfeiffer and Foster 2013, Igata et al. 2021).

In addition, spatial replays could be directed to non-goal locations where animals underwent fearful events or where they received satiated type of reward. Specifically, Wu et al. (2017) identified an imaginary spatial replay leading to the place where rats underwent an electric shock at the end of linear track, even though rats did not enter the shock zone. Carey et al. (2019) used different motivational states (i.e., thirsty or hungry) to bias the rat's navigation toward the choice arm containing the deprived reward (i.e., water or food) in the T-maze. They reported that replay occurred in the opposite direction relative to where the restricted reward was located, although rats shifted their behavior toward the restricted reward location. These results collectively suggest that the spatial replay of place cells in the dHP is modulated by spatial value information when different places are associated with positive or negative values in an environment.

Reactivation of place cells in the iHP coding high spatial values is potentiated by subsequent sleep

It is well known that neural firing patterns acquired during a recent experience are reactivated in the hippocampus during subsequent sleep. For example, two place cells whose fields overlap on the open arena exhibit an increased tendency to be reactivated together during the following sleep period (Wilson and McNaughton 1994). Also, the firing sequence of place cells during active behavior is observed again during reactivation in the post-sleep period (Lee and Wilson 2002). In the current study, we found that place cells coding high spatial values in the place-preference task had higher reactivation probabilities during SWRs, and they sustained their potentiated reactivation during subsequent post-sleep periods. The more frequent reactivation of motivationally salient information during sleep may facilitate the selective consolidation of such memories from the hippocampus to

neocortical networks. Consistent with this idea, we found a positive correlation between the amount of sleep reactivation of RM_{Hi} cells in the iHP and learning speed the next day. These results imply that higher-value spatial events are replayed more during post-behavioral sleep, presumably for their high priority during consolidation, and that learning on the next day may depend on such selective consolidation.

Acknowledgments

This study was supported by the National Research Foundation of Korea (NRF 2018R1A4A1025616, 2019R1A2C2088799, 2021R1A4A2001803, 2022M3E5E8017723, 2022R1I1A1A0106893511) and the BK21 FOUR supported by the Ministry of Education and NRF. We thank Joseph Shin for conducting certain pilot experiments for this study and aiding in the collection of electrophysiological data.

Author Contributions

J-S.W. designed the research, collected and analyzed the data, and wrote the manuscript. I.L. supervised all aspects of the research and wrote the manuscript.

Declaration of Interests

The authors declare no competing financial interests.

Figure Legends

Figure 1. Behavioral performance during the place-preference task

(A) Illustration of the place-preference task protocol. Rats started from the end of the south arm or north arm and were isolated at the ends of arms by an acrylic blocker between inter-trial intervals. The arms associated with high-value rewards and low-value rewards were reversed in Block 3 (blue shaded box). **(B and C)** Behavioral performance graph of sunflower seed (SS) vs. Cheerios (CR) session (rat 473 – session 2) and 4/4 SS vs. 1/4 SS session (rat 473 – session 3), based on a state-space model (Smith et al. 2004). High-value and low-value trials are marked by red and blue lines, respectively, above the learning curve. The solid black line indicates the estimated learning curve, and the black dashed line indicates the acquisition onset trial, calculated by the state-space model. The 90% confidence interval of the learning curve is shown by gray shading. **(D)** Boxplot for trials that reached acquisition onset for each block. **(E)** Boxplot presentation of mean latency per block. ***$p < 0.001$.

Figure 2. Detection of SWRs during the place-preference task

(A and B) Graphs of raw LFP, 150–250-Hz filtered signal, ensemble firing, and velocity illustrating the SWR periods that satisfied SWR criteria. SWR periods recorded from the iHP **(A)** and dHP **(B)** are indicated by gray-shaded areas. The scale indicates the amplitude of raw and filtered LFP signals. See also Figure S1. **(C)** Results for two individual rats exemplifying the distribution of SWR occurrence in the iHP and dHP. The black line indicates the contour of the maze; a spatial bin with lower SWR rates was excluded from the color display. SWRs recorded from Blocks 1 and 3 were pooled for calculation of the SWR rate map. See also Figure S2. **(D)** Pie chart showing the frequency of SWRs recorded from the dHP and iHP when rats were in the outbound zone, reward zone, inbound zone, and ITI zone during a place-preference task. ***$p < 0.001$.

Figure 3. Classification of place cells into four types

(A and B) Place cells in the iHP (A) and dHP (B) were divided into HiV and Lov based on the peak firing location of their place fields (i.e., High value and Low value). They were subsequently divided into non-remapping and remapping cells according to whether they remapped their field in response

to the reversal of reward value. Rate maps show peak firing rates above the rate maps, with the type of value associated with locations provided at the bottom of the rate map and between-rate map correlation coefficients shown between the rate maps. **(C)** Pie chart showing the number of NRM_{Hi}, RM_{Hi}, NRM_{Lo}, and RM_{Lo} place cells.

Figure 4. Exclusive reactivation of RM_{Hi} cells in the iHP during SWRs

(A) Examples of spatial rate maps for four cell types in the iHP. Cells #1-9 were ensemble cells observed in rat 473 – session 3. Rate maps show peak firing rates above the rate maps, with between-rate map correlation coefficients shown between rate maps. Spatial rate maps of nine single cells in the iHP are shown, together with their reactivation patterns during awake SWRs in Block 3. Spatial rate maps for each type are grouped as indicated by a colored box. Right panel: Examples of SWR and reactivation activities occurring after the reward value was changed. Raw LFP (i), 150–250-Hz filtered signals (ii), and reactivation of Cells #1-9 (iii) per SWR period are shown. Mean velocity during an SWR is shown on the raw LFP graph. The dashed line indicates the boundary of an SWR. **(B)** Box plot comparing the co-reactivation strength between RM_{Hi} cells and NRM_{Hi}, RM_{Hi}, NRM_{Lo}, and RM_{Lo} cells in the iHP. The strength of co-reactivation was calculated by dividing the number of co-reactivations for a given pair during an SWR by the number of reactivations in which either of the pairs was reactivated. **(C)** Comparison of reactivation probabilities in the iHP. Each dot indicates the reactivation probability of a single cell. See also Figure S3. *$p < 0.05$, **$p < 0.01$, ***$p < 0.001$.

Figure 5. Uniform reactivation of all cell types in the dHP

(A) Examples of spatial rate maps for four cell types in the dHP. Cells #1-8 were ensemble cells observed in rat 463 – session 1. Rate maps show peak firing rates above the rate maps, with between-rate map correlation coefficients indicated between the rate maps. Spatial rate maps of eight single cells in the dHP are presented, together with their reactivation patterns during an awake SWR in Block 3. Spatial rate maps of each type are grouped as indicated by a colored box. Right panel: Examples of SWRs and reactivation activities occurring after the reward value was changed. Raw LFP (i), 150–250-Hz filtered signals (ii), and reactivation of Cells #1-8 (iii) are shown for each SWR period. Mean velocity during an SWR is shown on the raw LFP graph. The dashed line indicates the boundary of an SWR. **(B)** Box plot comparing the co-reactivation strength between RM_{Hi} cells and

NRM_{Hi}, RM_{Hi}, NRM_{Lo}, and RM_{Lo} cells in the dHP. The strength of co-reactivation was calculated by dividing the number of co-reactivations for a given pair during an SWR by the number of reactivations in which either one of the pairs was reactivated. **(C)** Comparison of reactivation probabilities in the dHP. Each dot indicates the reactivation probability of a single cell. See also Figure S3.

Figure 6. Learning-dependent changes in the reactivation of RM_{Hi} cells in the iHP

(A and B) Examples of awake SWR and reactivation activities in the iHP (A) and (B) that occurred during correct and incorrect trials in the pre-learning state, and correct trials in the post-learning state. The single cells used in (A) and (B) are the same as those in Figure 4. Reactivation of NRM_{Hi}, RM_{Hi}, NRM_{Lo}, and RM_{Lo} cells are grouped by a color-shaded box. **(C and D)** Comparison of reactivation probabilities in the iHP among correct trials and incorrect trials in the pre-learning state and in the iHP **(C)** and dHP **(D)** among correct trials in post-learning trials. Each dot indicates the reactivation probability of a single cell; reactivation probabilities of the same cells are connected by a dashed line. See also Figure S4. *$p < 0.05$, ***$p < 0.001$.

Figure 7. Enhanced reactivation of RM_{Hi} cells in the iHP, but not in the dHP, is maintained during sleep after the place-preference task

(A and B) Examples of SWR and reactivation activities that occurred during pre-sleep and post-sleep in the iHP (A) and dHP (B). Raw LFP, 150–250-Hz filtered LFP, and reactivation of Cells #1-9 during the SWR period are shown. The single cells used to examine changes in reactivation activities in the post-sleep period compared with the pre-sleep period are the same as those used in Figure 4. Dashed line indicates the boundary of an SWR. **(C)** Box plot showing the inter-sleep co-reactivation difference, obtained by subtracting the reactivation probabilities of pre-sleep from those of post-sleep in the iHP and dHP. Each dot indicates the reactivation difference of one pair. **(D)** Comparison of inter-sleep reactivation differences among NRM_{Hi}, RM_{Hi}, NRM_{Lo}, and RM_{Lo} cells in the iHP and dHP. Each dot indicates the reactivation probability of a single cell. See also Figure S5. **(E)** Determining whether reactivation patterns show a positive relationship between behavior and sleep session by assessing the cross-correlation between the reactivation probabilities of RM_{Hi} cells in the iHP during a behavioral task and the sleep period. Each dot indicates the reactivation probability of a single cell. **(F)** Relationships between inter-sleep reactivation difference and

learning speed on the next day were examined based on the session mean reactivation probability in the iHP. Each dot represents the average of reactivation probabilities of RM_{Hi} cells per session. The dotted line indicates the 95% confidential interval of the linear regression. **(G and H)** The same analysis as in (E) and (F), applied in the dHP. See also Figure S6. $p < 0.05$, $^{**}p < 0.01$, $^{***}p < 0.001$.

Figure 8. Spatial replay leads towards the goal location in the dHP but not in the iHP
(A and B) Population rate maps of ensemble place cells constructed from the dHP (A) and iHP (B). **(C and D)** Individual examples of SWRs and replay that occurred during occupation of the reward zone. 150–250-Hz filtered LFP, reactivated spikes, and posterior probability of decoded position during an SWR are shown. The boundary of the SWR is indicated by a black dashed line; the calculated linear regression line is indicated by a red dashed line; and the statistical significance of permutation tests is denoted by an asterisk. **(E)** Pie chart showing the proportion of significant replay events between the dHP and iHP that occurred during occupation of the reward zone. The numbers of significant replays and candidate replay events are denoted in the bar. **(F)** The proportion of significant replays representing trajectories that lead to high-value or low-value rewards depending on the trial type. $^{**}p < 0.01$.

STAR Methods

KEY RESOURCE TABLE

Provided in a separate file

LEAD CONTACT AND MATERIAL AVAILABILITY

Further information and requests for resources and materials should be directed to and will be fulfilled by the Lead Contact, Inah Lee (inahlee@snu.ac.kr).

Subjects

Six male Long-Evans rats weighing 300-400 g were used. Food was restricted to maintain body weight at 85% of free-feeding weight to sustain a higher motivation level in behavioral tasks; water was available ad libitum. Animals were housed individually under a 12-hour light/dark cycle. All protocols and procedures conformed to the guidelines of the Institutional Animal Care and Use Committee (IACUC) of Seoul National University.

Behavior paradigm

Place-preference task (T-maze). An 8-arm maze (central platform size, 401 cm^2; arm size, 8 × 45 cm; height, 70 cm from the floor) was converted to a T-maze by installing a T-shaped transparent acrylic structure in the center platform. The rat was confined to the start arm by an acrylic blocker. A food well (2 cm in diameter and 8 mm in depth) was located at the end of each arm, with a proximity sensor installed underneath the well to detect the displacement of an acrylic disc (2.5 cm in diameter) that covered the food well. An infrared sensor was installed at each arm entry. Transistor-transistor logic (TTL) sensor signals were transmitted to a data-acquisition system (Digital Lynx SX; Neuralynx). An LED-light complex to illuminate the experimental room and digital cameras to monitor animals' positions were installed on the ceiling. The maze was surrounded by circular black curtains to which a considerable number of visual cues were attached. White noise (80 dB) was delivered through two loudspeakers during the recording session to mask unwanted noise in the environment. In the place-preference task, rats were required to choose an arm baited with a more preferred type of reward (i.e., sunflower seeds [SS] or whole sunflower seeds [4/4 SS]) over a less-preferred reward (i.e., Cheerios cereal [CR] or quarter sunflower seeds [1/4 SS]). Rats initially

learned the arm in which the more preferred reward was baited by trial and error in Block 1. In Block 2, rats were started from the opposite start arm to make the task more hippocampal-dependent (Packard and McGaugh 1996). In Block 3, they started from the original starting arm but the locations associated with higher-value and lower-value rewards were reversed. This experimental design sought to examine the rat's behavior and neural correlates when updating place and its associated value in the environment (Figure 1A). Each block was terminated when rats chose the arm baited with the preferred reward more than 12 times in the previous 15 trials. After the rats had been tested for 2 days with SS and CR rewards, they were tested in the same task, but this time were provided the preferred type of reward (SS) only in the two reward arms but in different amounts (i.e., 4/4 SS vs. 1/4 SS). The higher-value location on the first day was pseudo-randomly determined, and all rats departed from the south arm in Block 1. The location of the high-value location the next day was the same as that of the last high-value location the day before.

Maze pre-training and surgery

After rats had become familiarized with the maze environment for a few days (30 min/d), they were trained in a shuttling task in which they alternated between the two adjacent arms of the 8-arm maze to obtain rewards. Rats were trained to complete 240 trials in 1 hour, which took approximately 4 days (mean, 3.8 days; SD, 1.1 days). After pre-training, a hyperdrive containing 24 tetrodes was implanted for recording spikes from single units and local field potentials (LFPs). Tetrodes were made using platinum wires (17.8 μm in diameter). A semi-automatic plating device (Nano-Z; Neuralynx) was used to adjust the final impedance of each tetrode to approximately 130 kΩ (measured in gold solution at 1 kHz). The hyperdrive was configured to have two separate electrode bundles, one carrying 18 tetrodes to target the iHP and vHP (coordinates for implantation: 5 mm posterior to bregma, 6 mm lateral from midline), and the other containing 6 tetrodes to target the dHP (coordinates for implantation: 3.2 mm posterior to bregma, 3 mm lateral from midline). The bundles were inserted obliquely (5 degrees medially from the vertical axis) into the hyperdrive frame so that the tetrodes could maximally target the cell layers in the iHP.

Post-surgical training and main recordings

After 1 week of recovery from surgery, rats were retrained in the shuttling task. Retraining of rats to the same pre-surgical criterion required 10 ± 3 days (mean ± SD). During the post-training period,

tetrodes were gradually lowered into the CA1 cell layer in the hippocampus while the rat was at rest on a pedestal. Once most tetrodes reached their target cell layers in the dorsal and intermediate-ventral regions in the hippocampus, the main recordings began. Place cell activity was recorded while rats shuttled on the two adjacent arms (spatial alternation task) for 7 days according to a previously detailed experimental protocol (Jin and Lee 2021). On days 8 to 11, rats performed the place-preference task in the T-maze. SS and CR were used as high-value and low-value rewards for recording on days 8 and 9, respectively, and 4/4 SS (high value) and 1/4 SS (low value) were utilized for days 10 and 11, respectively. Sleep sessions were recorded for approximately 30 minutes before and after the place-preference task while rats were at rest or asleep.

Electrophysiological recording procedures

After 1 week of recovery, each rat was placed on a custom-built pedestal outside the experimental room and habituated to rest for tetrode adjustment. Tetrodes were lowered individually to the cell layers over ~2 weeks. Neural activity was amplified (1,000-10,000 times) and digitized (sampling frequency, 32 kHz; filtered at 600-6,000 Hz for spiking data and 0.1-1,000 Hz for LFP) using a Digital Lynx system (Neuralynx). The rat's position and head direction were measured using an array of red and green LEDs attached to a custom headstage complex coupled to a preamplifier (HS-36; Neuralynx). A ceiling camera recorded LED positions and fed the signal to a frame grabber (sampling frequency, 30 Hz).

Histological verification of electrode tracks

After completion of the main recording sessions, tetrode-tip locations were marked by passing a weak electrical current through each tetrode (10 μA for 10 s). On the next day, the rat was sacrificed using an overdose of carbon dioxide (CO_2) and then was perfused transcardially, first with phosphate-buffered saline (PBS) and then with a 4% (v/v) formaldehyde solution. Thereafter, the brain was removed and kept in a 4% v/v formaldehyde-30% sucrose solution at 4°C until it sank. The brain was sectioned in the coronal plane at 40-μm thickness using a sliding microtome (HM 430; Thermo-Fisher Scientific), mounted on a slide glass, and then stained with thionin. Photomicrographs were taken using a digital camera attached to a microscope (Eclipse 80i; Nikon). Tetrode tracks were reconstructed using a series of sections, taking into account the presurgical configuration of the tetrode-array bundle and electrolytic lesion marks. Dorsoventral (DV) recording

positions of place cells were quantitatively measured as the vertical distance from the cortical surface to electrode tip locations.

Data analysis

Unit isolation

Spikes associated with single units were isolated using a Windows-based, custom-written program (WinClust). The parameters, peak, valley, energy, and spike width, calculated from waveforms recorded from the four channels of a tetrode, were used for isolation. Unit-isolation quality was evaluated during cluster-cutting procedures, with each cluster defined as isolation quality 1 (poorly isolated) to 5 (well isolated) based on how well the cluster was separated from neighboring clusters and background noise. Units with an isolation rating of 1 were excluded from further analysis. Inter-spike interval (ISI) histograms were also used to judge the quality of the cut cluster. Units showing a mean firing rate > 10 Hz (either in the open field or in the radial maze) with a spike width < 300 μs were classified as inhibitory interneurons and were excluded from further analysis.

Sharp-wave ripple detection

SWRs were extracted from local field potentials (LFPs) using the following steps. First, the two tetrodes that recorded the largest SWRs were selected and the corresponding LFP signals were filtered with a 150-250 Hz bandpass filter. Sections exceeding 4 SDs from the average of the filtered signals were initially selected, and the point where enhanced signals decreased by less than 1 SD was taken as the boundary of the SWR for each tetrode. The SWR boundary was determined as the sum of the SWR boundaries of two tetrodes. If only one tetrode exceeded the threshold within a particular section, it was not counted as an SWR. Next, the number of cells reactivated within the SWR boundary was measured. If the number of reactivated cells was less than 5% of the total number of recorded cells, the signal was considered noise. Finally, signals recorded during passage of an SWR boundary were also considered noise if the animal's head movement speed at the time was > 20 cm/s (e.g., bumping noise due to collision with the acrylic blocker installed in the T-maze).

Basic firing properties

To construct a rate map, we first scaled the 720 × 480 pixel space down to 72 × 48 pixel space (1 pixel = 2 × 2 cm). The firing rate associated with a given pixel was calculated by dividing the number of visits by the number of spikes fired in each pixel. The raw rate map was then smoothed using an adaptive binning method. The amount of spatial information associated with a single spike of a single unit was measured by calculating spatial information based on the firing rate map, according to the following equation (Skaggs et al. 1992):

$$\text{Spatial information} = \sum p_i \frac{\lambda_i}{\lambda} log_2 \frac{\lambda_i}{\lambda} \left(\frac{bit}{spike}\right),$$

where i denotes bin, p_i is the occupancy rate in the ith bin, λ_i indicates the mean firing rate in the ith bin, and λ is the overall mean firing rate. Stability within the square box test was measured by comparing the firing rate map between the first half and the second half of the session using Pearson's correlation.

Behavior analysis

For learning curve analyses, we calculated the estimated learning curve and the trial at which the rat reaches acquisition onset by applying a state-space model to behavioral performance (Smith et al. 2004). Latency is the time elapsed from passing by the infrared sensor installed at the entry of the start arm to reaching the food well. Learning speed is the inverse value of the trials to reach the learning criterion. In Figure 7F and 7H, we measured the learning speed in Block 1 on the next day. Because the high-value location of the first block on the day of the experiment was the same as the last block on the previous day, faster learning by rats in the first block was taken to mean that the information of high-value locations was strongly strengthened by sleep reactivation of high-value-coding place cells in the iHP.

Place cell analysis

A place cell was defined by applying the following steps. First, the spatial rate map, smoothed using Skaggs's adaptive binning method, was calculated, and the pixel with the maximal firing rate was identified. Then, the firing rates associated with all other pixels were compared against the maximal firing rate, and only those pixels whose firing rate exceeded 20% of the peak firing rate were retained for further analysis. Among the remaining pixels, one or more sets of continuous pixels

(>40 cm^2 in size with a peak firing rate > 1 Hz) were defined as place fields. In cases where multiple place fields were found during the procedure, the field size of the unit was calculated by taking the sum of all subfields as the unit's field size. Spiking data were included only if instantaneous speeds were greater than 5 cm/s at the time of the spike; spikes in the reward zones were excluded from the analysis (Lee et al. 2006). Because a proximity sensor was installed inside the food well, the exact timestamp when rats displaced the disc covering the reward could be measured. A cell was operationally defined as a place cell if 1) its field size was greater than 40 cm^2, and its peak and mean firing rates were greater than 1 Hz and 0.25 Hz, respectively, and 3) its spatial information was higher than 0.25 bits/spike with a statistical significance of $p < 0.01$(Skaggs et al. 1992, Lee et al. 2004).

Place cells were divided into non-remapping and remapping place cells based on Pearson's correlation coefficient (R) of spatial rate maps between Block 1 and Block 3. If R was greater than 0.75, it was regarded as a non-remapping place cell; otherwise, it was classified as a remapping place cell (Figure 3).

Reactivation analysis

Co-reactivation probability, reactivation probability, and reactivation rate were calculated using SWR events that occurred in Block 3, where location- and value-coding place cells were best dissociated. Co-reactivation probability, which corresponds to the probability that two place cells were reactivated together, was measured by dividing the number of SWRs in which both place cells constituting a pair were reactivated by the number of SWRs in which at least one of the two cells was reactivated. Reactivation probability was calculated by dividing the number of SWRs in which one place cell was reactivated by the total number of SWRs. Reactivation rate was measured by dividing the number of total reactivated spikes by the sum of total SWR durations. The same calculations were applied to pre- and post-sleep sessions, and the entire (~30 min) pre- and post-sleep dataset was used for calculating reactivation activities.

Constructing the population rate map

Population rate maps for the place-preference task were constructed by linearizing spatial rate maps for all place cells and stacking them (bin size = 2 cm). Trials performed after reaching acquisition

onset in Block 3 were used to create a spatial rate map, and the population rate map was created using Block 3. The firing rate in each bin was calculated by dividing the number of spikes by the number of occupancies by the rat within that bin. In the curved section, a fan-shaped boundary with an internal angle of 22.5 degrees was defined as a bin. Linearized firing rate maps were smoothed using a Gaussian window (window size, 22 cm; full width at half maximum [FWHM], 10 cm).

Bayesian decoding for position reconstruction

The rat's positional information was reconstructed from the activity of place cells by applying a Bayesian decoding algorithm (Zhang et al. 1998, Brown et al. 1998). In Bayesian analysis, value-coding place cells, location-coding place cells, and place cells whose fields were located in the stem of the T-maze were pooled. Briefly, the number of spikes at a given time $\boldsymbol{t}$, $n_i(\boldsymbol{t})$, was calculated for each place cell, i. The 2D spatial rate map was linearized to a 1D spatial rate map and the mean firing rate at given spatial position $\boldsymbol{x}$, $\boldsymbol{\lambda}_i(\boldsymbol{x})$, was calculated. The reconstruction was obtained using two vectors, $\boldsymbol{n}(\boldsymbol{t}) = (n_1, n_2, \dots n_N)$ and $\boldsymbol{\lambda}(\boldsymbol{x}) = (\lambda_1, \lambda_2, \dots \lambda_N)$, where 'N' is the number of recorded place cells and the firing probability was assumed to follow a Poisson distribution.

The animal's position was reconstructed using the standard formula for conditional probability (1):

$$\mathrm{P}(\boldsymbol{x}/\boldsymbol{n})\mathrm{P}(\boldsymbol{n}) = \mathrm{P}(\boldsymbol{n}/\boldsymbol{x})\mathrm{P}(\boldsymbol{x}) \quad \cdots \quad (1)$$

where $\mathrm{P}(\boldsymbol{x})$ is the probability that the animal is positioned at $\boldsymbol{x}$, and $\mathrm{P}(\boldsymbol{x}/\boldsymbol{n})$ is the conditional probability that the animal is located at position $\boldsymbol{x}$ when the spike count was $\boldsymbol{n}$. This equation (1) is rearranged to (2) to solve for conditional probability of reconstructed animal's position.

$$\mathrm{P}(\boldsymbol{x}/\boldsymbol{n}) = \frac{\mathrm{P}(\boldsymbol{n}/\boldsymbol{x})\mathrm{P}(\boldsymbol{x})}{\mathrm{P}(\boldsymbol{n})} \quad \cdots \quad (2)$$

Assuming that the firing characteristics of each place cells follow a Poisson distribution and that all cells fire independently, the prior template, $\mathrm{P}(\boldsymbol{n}/\boldsymbol{x})$, was calculated as (3):

$$\mathrm{P}(\boldsymbol{n}/\boldsymbol{x}) = \prod_{i=1}^{N} \mathrm{P}(n_i/\boldsymbol{x}) = \prod_{i=1}^{N} \frac{(\tau\lambda_i(\boldsymbol{x}))^{n_i}}{n_i!} exp(-\tau\lambda_i(\boldsymbol{x})) \quad \cdots \quad (3)$$

where τ is the time window for data sampling (20 ms). Thus, $\mathrm{P}(\boldsymbol{x}/\boldsymbol{n})$ was calculated according to

the equation (4):

$$\mathrm{P}(\boldsymbol{x}/\boldsymbol{n}) = \frac{\prod_{i=1}^{N}\left(\frac{(\tau\lambda_i(\boldsymbol{x}))^{n_i}}{n_i!}\right) exp(-\tau\sum_{i=1}^{N}\lambda_i(\boldsymbol{x}))\, P(\boldsymbol{x})}{\mathrm{P}(\boldsymbol{n})} \quad \cdots \quad (4)$$

and $\mathrm{P}(\boldsymbol{n})$ was used to normalize probabilities (Zhang et al., 1998). The position at which $\mathrm{P}(\boldsymbol{x}/\boldsymbol{n})$ was maximum was considered to be the reconstructed position ($\widehat{\boldsymbol{x}}$):

$$\widehat{\boldsymbol{x}} = argmax\ \mathrm{P}(\boldsymbol{x}/\boldsymbol{n})$$

QUANTIFICATION AND STATISTICAL ANALYSIS

Statistical testing was performed with MATLAB using built-in and custom-made functions. The null hypothesis was rejected using the non-parametric Wilcoxon rank-sum and Kruskal-Wallis tests. A Chi-square test was utilized to test the proportional difference between groups. The significance of linear relationships between two dependent variables was tested using linear regression. A Bonferroni correction was used to correct the significance level. Statistical results are reported in the Results sections. All tests were two-tailed, and significance was accepted at a p-value of 0.05.

DATA AND CODE AVAILABILITY

Data and MATLAB code are available from the authors upon reasonable request.

SUPPLEMENTARY TABLE AND VIDEO

Video S1. A rat performing a place-preference task; Related to Figure 1

Reference

Ambrose, R. E., Pfeiffer, B. E. and Foster, D. J. (2016) 'Reverse Replay of Hippocampal Place Cells Is Uniquely Modulated by Changing Reward', *Neuron,* 91(5), 1124-36.

Bast, T., Wilson, I. A., Witter, M. P. and Morris, R. G. (2009) 'From rapid place learning to behavioral performance: a key role for the intermediate hippocampus', *PLoS Biol,* 7(4), e1000089.

Bhattarai, B., Lee, J. W. and Jung, M. W. (2020) 'Distinct effects of reward and navigation history on hippocampal forward and reverse replays', *Proc Natl Acad Sci U S A,* 117(1), 689-697.

Brown, E. N., Frank, L. M., Tang, D., Quirk, M. C. and Wilson, M. A. (1998) 'A statistical paradigm for neural spike train decoding applied to position prediction from ensemble firing patterns of rat hippocampal place cells', *J Neurosci,* 18(18), 7411-25.

Burton, B. G., Hok, V., Save, E. and Poucet, B. (2009) 'Lesion of the ventral and intermediate hippocampus abolishes anticipatory activity in the medial prefrontal cortex of the rat', *Behav Brain Res,* 199(2), 222-34.

Buzsaki, G. (1989) 'Two-stage model of memory trace formation: a role for "noisy" brain states', *Neuroscience,* 31(3), 551-70.

Carey, A. A., Tanaka, Y. and van der Meer, M. A. A. (2019) 'Reward revaluation biases hippocampal replay content away from the preferred outcome', *Nat Neurosci,* 22(9), 1450-1459.

De Saint Blanquat, P., Hok, V., Save, E., Poucet, B. and Chaillan, F. A. (2013) 'Differential role of the dorsal hippocampus, ventro-intermediate hippocampus, and medial prefrontal cortex in updating the value of a spatial goal', *Hippocampus,* 23(5), 342-51.

Diba, K. and Buzsaki, G. (2007) 'Forward and reverse hippocampal place-cell sequences during ripples', *Nat Neurosci,* 10(10), 1241-2.

Duvelle, E., Grieves, R. M., Hok, V., Poucet, B., Arleo, A., Jeffery, K. and Save, E. (2019) 'Insensitivity of place cells to the value of spatial goals in a two-choice flexible navigation task', *J Neurosci*.

Eichenbaum, H. (2000) 'A cortical-hippocampal system for declarative memory', *Nat Rev Neurosci,* 1(1), 41-50.

Eichenbaum, H. and Cohen, N. J. (2001) *From conditioning to conscious recollection: Memory systems of the brain, From conditioning to conscious recollection: Memory systems of the brain.*, New York, NY, US: Oxford University Press.

Foster, D. J. and Wilson, M. A. (2006) 'Reverse replay of behavioural sequences in hippocampal place cells during the awake state', *Nature*, 440(7084), 680-3.

Gauthier, J. L. and Tank, D. W. (2018) 'A Dedicated Population for Reward Coding in the Hippocampus', *Neuron*, 99(1), 179-193.e7.

Gillespie, A. K., Astudillo Maya, D. A., Denovellis, E. L., Liu, D. F., Kastner, D. B., Coulter, M. E., Roumis, D. K., Eden, U. T. and Frank, L. M. (2021) 'Hippocampal replay reflects specific past experiences rather than a plan for subsequent choice', *Neuron*.

Igata, H., Ikegaya, Y. and Sasaki, T. (2021) 'Prioritized experience replays on a hippocampal predictive map for learning', *Proc Natl Acad Sci U S A*, 118(1).

Jarzebowski, P., Hay, Y. A., Grewe, B. F. and Paulsen, O. (2022) 'Different encoding of reward location in dorsal and intermediate hippocampus', *Current Biology*.

Jin, S. W. and Lee, I. (2021) ' Differential encoding of place value between the dorsal and intermediate hippocampus', *Curr Biol*.

Jung, M. W., Wiener, S. I. and McNaughton, B. L. (1994) 'Comparison of spatial firing characteristics of units in dorsal and ventral hippocampus of the rat', *J Neurosci*, 14(12), 7347-56.

Karlsson, M. P. and Frank, L. M. (2009) 'Awake replay of remote experiences in the hippocampus', *Nat Neurosci*, 12(7), 913-918.

Kjelstrup, K. B., Solstad, T., Brun, V. H., Hafting, T., Leutgeb, S., Witter, M. P., Moser, E. I. and Moser, M. B. (2008) 'Finite scale of spatial representation in the hippocampus', *Science*, 321(5885), 140-3.

Lee, A. K. and Wilson, M. A. (2002) 'Memory of sequential experience in the hippocampus during slow wave sleep', *Neuron*, 36(6), 1183-94.

Lee, I., Griffin, A. L., Zilli, E. A., Eichenbaum, H. and Hasselmo, M. E. (2006) 'Gradual translocation of spatial correlates of neuronal firing in the hippocampus toward prospective reward locations', *Neuron*, 51(5), 639-50.

Lee, I., Yoganarasimha, D., Rao, G. and Knierim, J. J. (2004) 'Comparison of population coherence of place cells in hippocampal subfields CA1 and CA3', *Nature,* 430(6998), 456-9.

Michon, F., Sun, J. J., Kim, C. Y., Ciliberti, D. and Kloosterman, F. (2019) 'Post-learning Hippocampal Replay Selectively Reinforces Spatial Memory for Highly Rewarded Locations', *Curr Biol,* 29(9), 1436-1444.e5.

Moita, M. A., Rosis, S., Zhou, Y., LeDoux, J. E. and Blair, H. T. (2004) 'Putting fear in its place: remapping of hippocampal place cells during fear conditioning', *J Neurosci,* 24(31), 7015-23.

Mou, X., Pokhrel, A., Suresh, P. and Ji, D. (2022) 'Observational learning promotes hippocampal remote awake replay toward future reward locations', *Neuron,* 110(5), 891-902.e7.

Ormond, J., Serka, S. A. and Johansen, J. P. (2023) 'Enhanced reactivation of remapping place cells during aversive learning', *The Journal of Neuroscience,* JN-RM-1450-22.

Packard, M. G. and McGaugh, J. L. (1996) 'Inactivation of hippocampus or caudate nucleus with lidocaine differentially affects expression of place and response learning', *Neurobiol Learn Mem,* 65(1), 65-72.

Pfeiffer, B. E. and Foster, D. J. (2013) 'Hippocampal place-cell sequences depict future paths to remembered goals', *Nature,* 497(7447), 74-9.

Singer, A. C. and Frank, L. M. (2009) 'Rewarded outcomes enhance reactivation of experience in the hippocampus', *Neuron,* 64(6), 910-21.

Skaggs, McNaughton, B. L., Gothard, K. M. and Markus, E. J. (1992) 'An Information-Theoretic Approach to Deciphering the Hippocampal Code', *Proceedings of the 5th International Conference on Neural Information Processing Systems,* 1030–1037.

Smith, A. C., Frank, L. M., Wirth, S., Yanike, M., Hu, D., Kubota, Y., Graybiel, A. M., Suzuki, W. A. and Brown, E. N. (2004) 'Dynamic Analysis of Learning in Behavioral Experiments', *The Journal of Neuroscience,* 24(2), 447-461.

Squire, L. R., Stark, C. E. and Clark, R. E. (2004) 'The medial temporal lobe', *Annu Rev Neurosci,* 27, 279-306.

Tabuchi, E., Mulder, A. B. and Wiener, S. I. (2003) 'Reward value invariant place responses and

reward site associated activity in hippocampal neurons of behaving rats', *Hippocampus*, 13(1), 117-32.

Widloski, J. and Foster, D. J. (2022) 'Flexible rerouting of hippocampal replay sequences around changing barriers in the absence of global place field remapping', *Neuron*.

Wilson, M. A. and McNaughton, B. L. (1994) 'Reactivation of hippocampal ensemble memories during sleep', *Science*, 265(5172), 676-9.

Wu, C. T., Haggerty, D., Kemere, C. and Ji, D. (2017) 'Hippocampal awake replay in fear memory retrieval', *Nat Neurosci*, 20(4), 571-580.

Zhang, K., Ginzburg, I., McNaughton, B. L. and Sejnowski, T. J. (1998) 'Interpreting neuronal population activity by reconstruction: unified framework with application to hippocampal place cells', *J Neurophysiol*, 79(2), 1017-44.

Figure 1

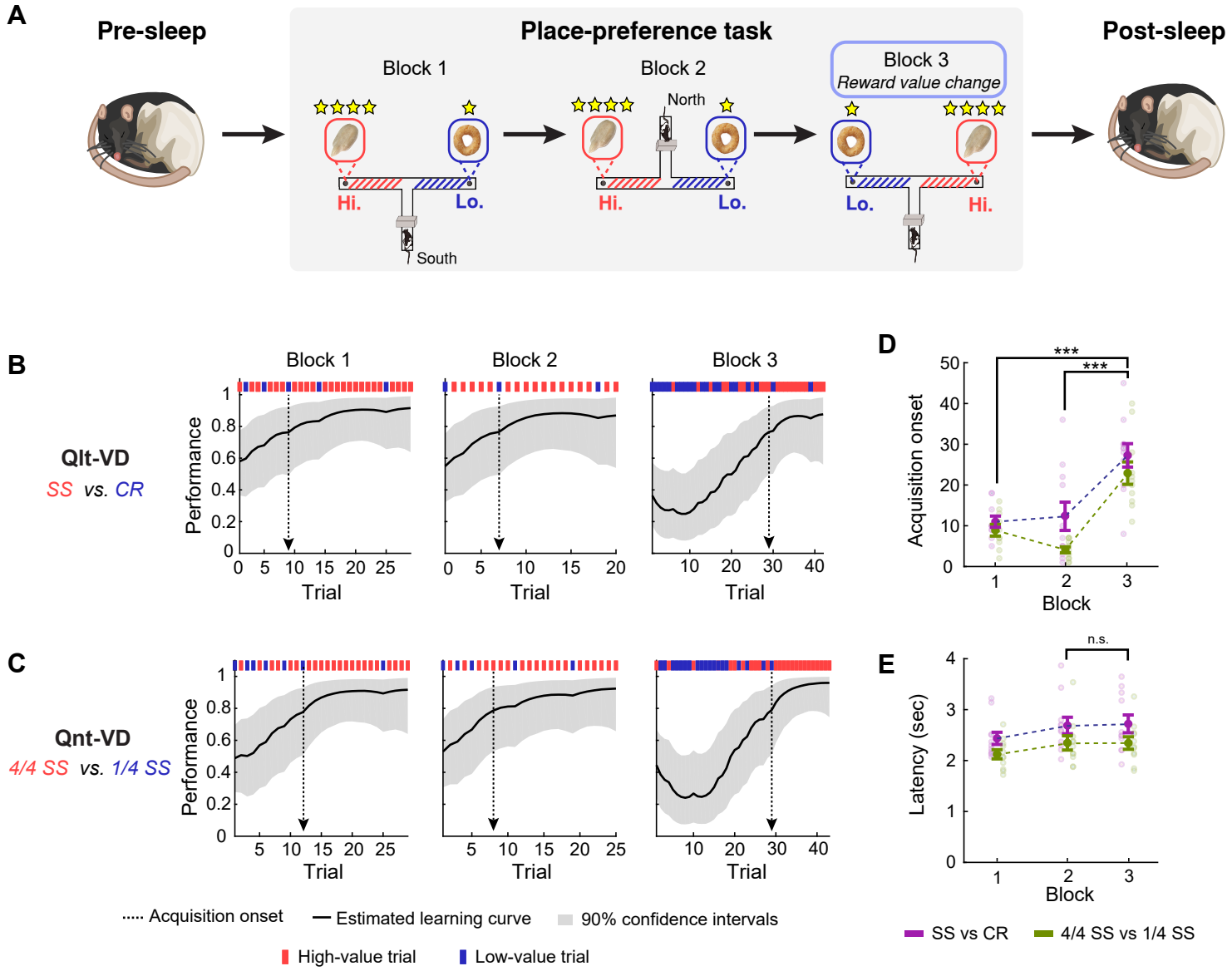
A
Pre-sleep
Place-preference task
Block 1
Block 2
Block 3
Reward value change
North
South
Hi.
Lo.
Post-sleep
B
Block 1
Block 2
Block 3
QIt-VD
SS vs. CR
Performance
Trial
C
Qnt-VD
4/4 SS vs. 1/4 SS
D
Acquisition onset
Block
***
E
Latency (sec)
n.s.
Acquisition onset
Estimated learning curve
90% confidence intervals
High-value trial
Low-value trial
SS vs CR
4/4 SS vs 1/4 SS

Figure 2

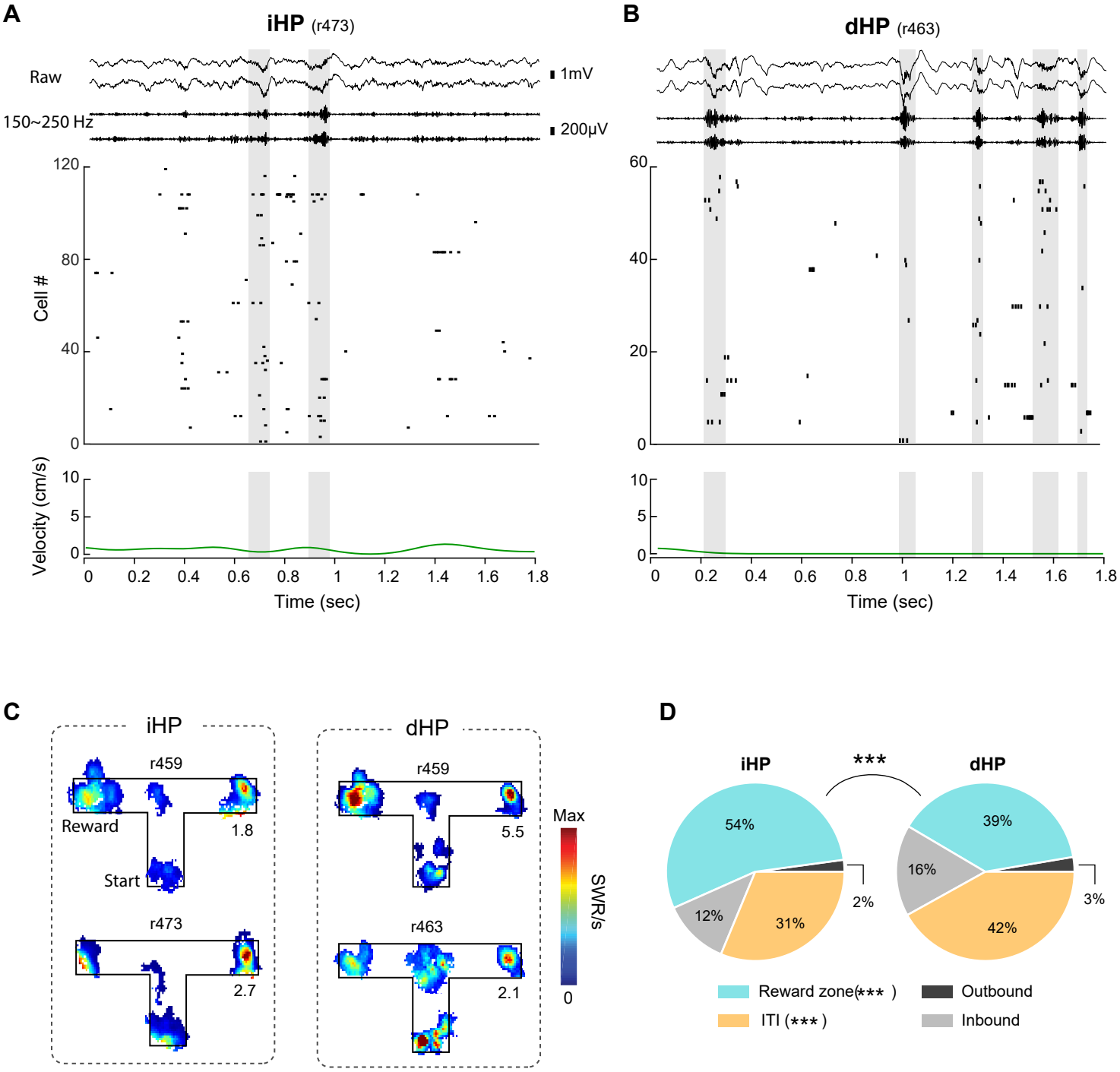
A
iHP (r473)
Raw
150~250 Hz
1mV
200μV
Cell #
Velocity (cm/s)
Time (sec)
B
dHP (r463)
Time (sec)
C
iHP
r459
Reward
1.8
Start
r473
2.7
dHP
r459
5.5
r463
2.1
Max
SWR/s
0
D
iHP
***
dHP
54%
2%
12%
31%
39%
16%
3%
42%
Reward zone(***)
ITI (***)
Outbound
Inbound

Figure 3

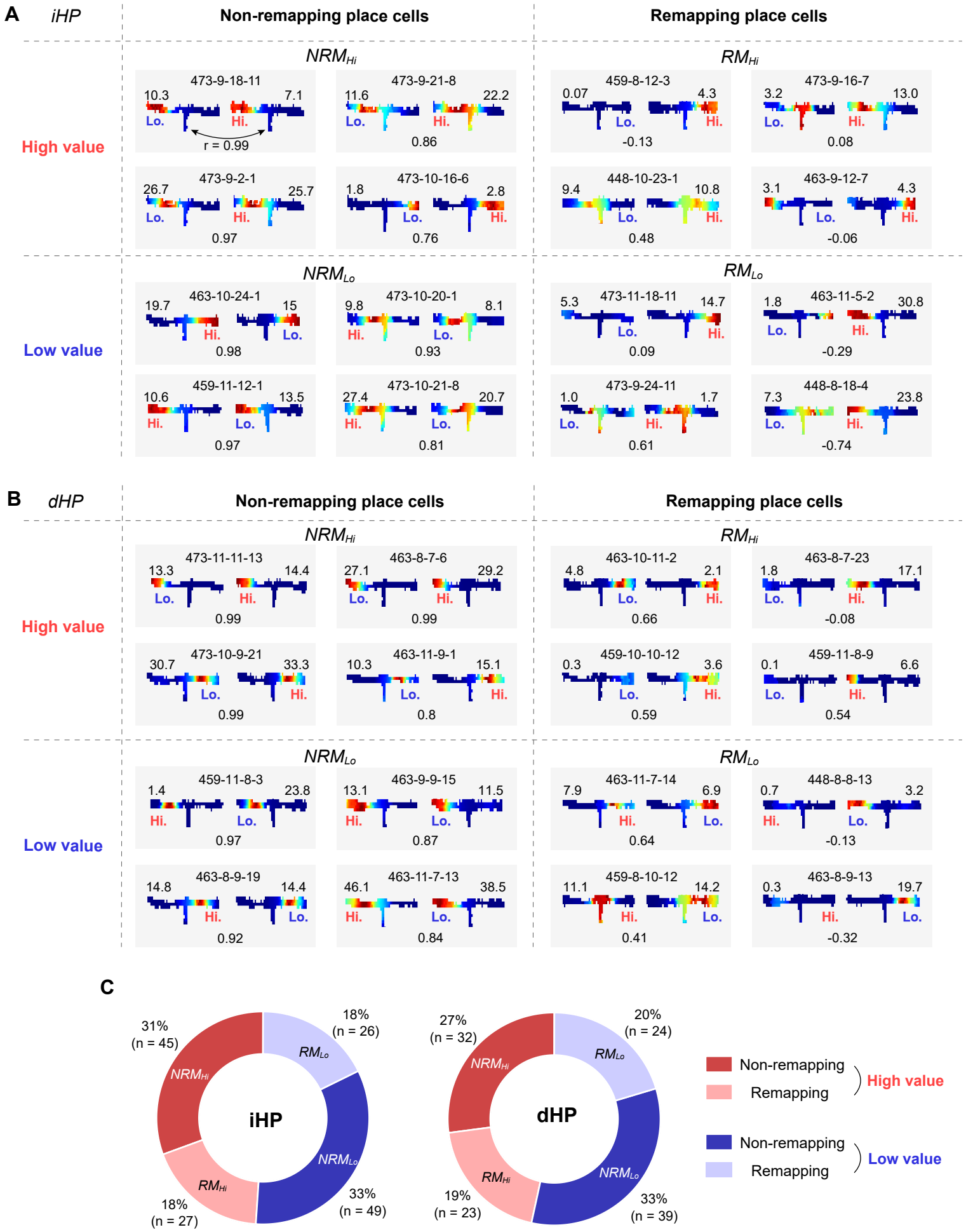
A
iHP
Non-remapping place cells
Remapping place cells
High value
Low value
NRMHi
RMHi
NRMLo
RMLo
473-9-18-11
10.3
7.1
Lo.
Hi.
r = 0.99
473-9-21-8
11.6
22.2
0.86
459-8-12-3
0.07
4.3
-0.13
473-9-16-7
3.2
13.0
0.08
473-9-2-1
26.7
25.7
0.97
473-10-16-6
1.8
2.8
0.76
448-10-23-1
9.4
10.8
0.48
463-9-12-7
3.1
4.3
-0.06
463-10-24-1
19.7
15
0.98
473-10-20-1
9.8
8.1
0.93
473-11-18-11
5.3
14.7
0.09
463-11-5-2
1.8
30.8
-0.29
459-11-12-1
10.6
13.5
0.97
473-10-21-8
27.4
20.7
0.81
473-9-24-11
1.0
1.7
0.61
448-8-18-4
7.3
23.8
-0.74
B
dHP
Non-remapping place cells
Remapping place cells
High value
Low value
NRMHi
RMHi
NRMLo
RMLo
473-11-11-13
13.3
14.4
0.99
463-8-7-6
27.1
29.2
0.99
463-10-11-2
4.8
2.1
0.66
463-8-7-23
1.8
17.1
-0.08
473-10-9-21
30.7
33.3
0.99
463-11-9-1
10.3
15.1
0.8
459-10-10-12
0.3
3.6
0.59
459-11-8-9
0.1
6.6
0.54
459-11-8-3
1.4
23.8
0.97
463-9-9-15
13.1
11.5
0.87
463-11-7-14
7.9
6.9
0.64
448-8-8-13
0.7
3.2
-0.13
463-8-9-19
14.8
14.4
0.92
463-11-7-13
46.1
38.5
0.84
459-8-10-12
11.1
14.2
0.41
463-8-9-13
0.3
19.7
-0.32
C
31%
(n = 45)
18%
(n = 26)
18%
(n = 27)
33%
(n = 49)
iHP
27%
(n = 32)
20%
(n = 24)
19%
(n = 23)
33%
(n = 39)
dHP
Non-remapping
Remapping
High value
Non-remapping
Remapping
Low value

Figure 4

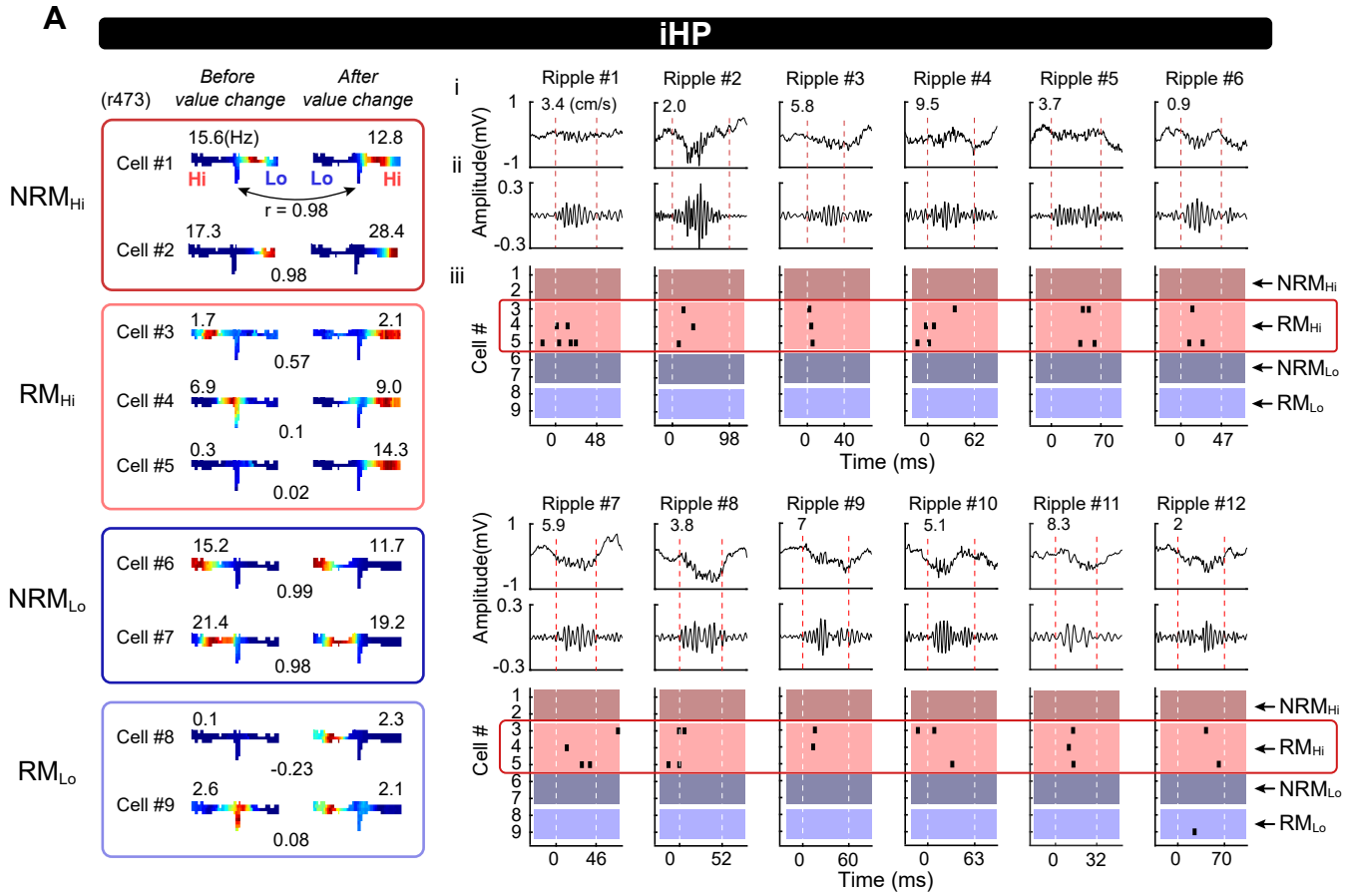
A
iHP
(r473)
Before value change
After value change
NRMHi
Cell #1
15.6(Hz)
12.8
Hi
Lo
Lo
Hi
r = 0.98
Cell #2
17.3
28.4
0.98
RMHi
Cell #3
1.7
2.1
0.57
Cell #4
6.9
9.0
0.1
Cell #5
0.3
14.3
0.02
NRMLo
Cell #6
15.2
11.7
0.99
Cell #7
21.4
19.2
0.98
RMLo
Cell #8
0.1
2.3
-0.23
Cell #9
2.6
2.1
0.08
i
ii
iii
Ripple #1
Ripple #2
Ripple #3
Ripple #4
Ripple #5
Ripple #6
3.4 (cm/s)
2.0
5.8
9.5
3.7
0.9
Amplitude(mV)
Cell #
Time (ms)
Ripple #7
Ripple #8
Ripple #9
Ripple #10
Ripple #11
Ripple #12
5.9
3.8
7
5.1
8.3
2
NRMHi
RMHi
NRMLo
RMLo

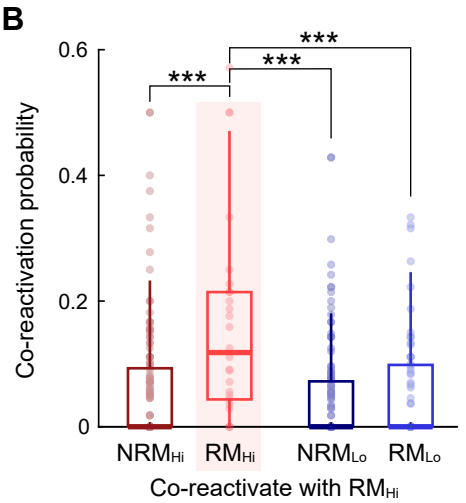
B
Co-reactivation probability
***
***
***
NRMHi
RMHi
NRMLo
RMLo
Co-reactivate with RMHi

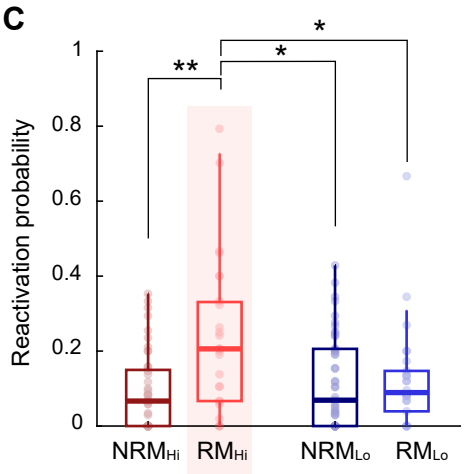
C
Reactivation probability
**
*
*
NRMHi
RMHi
NRMLo
RMLo

Figure 5

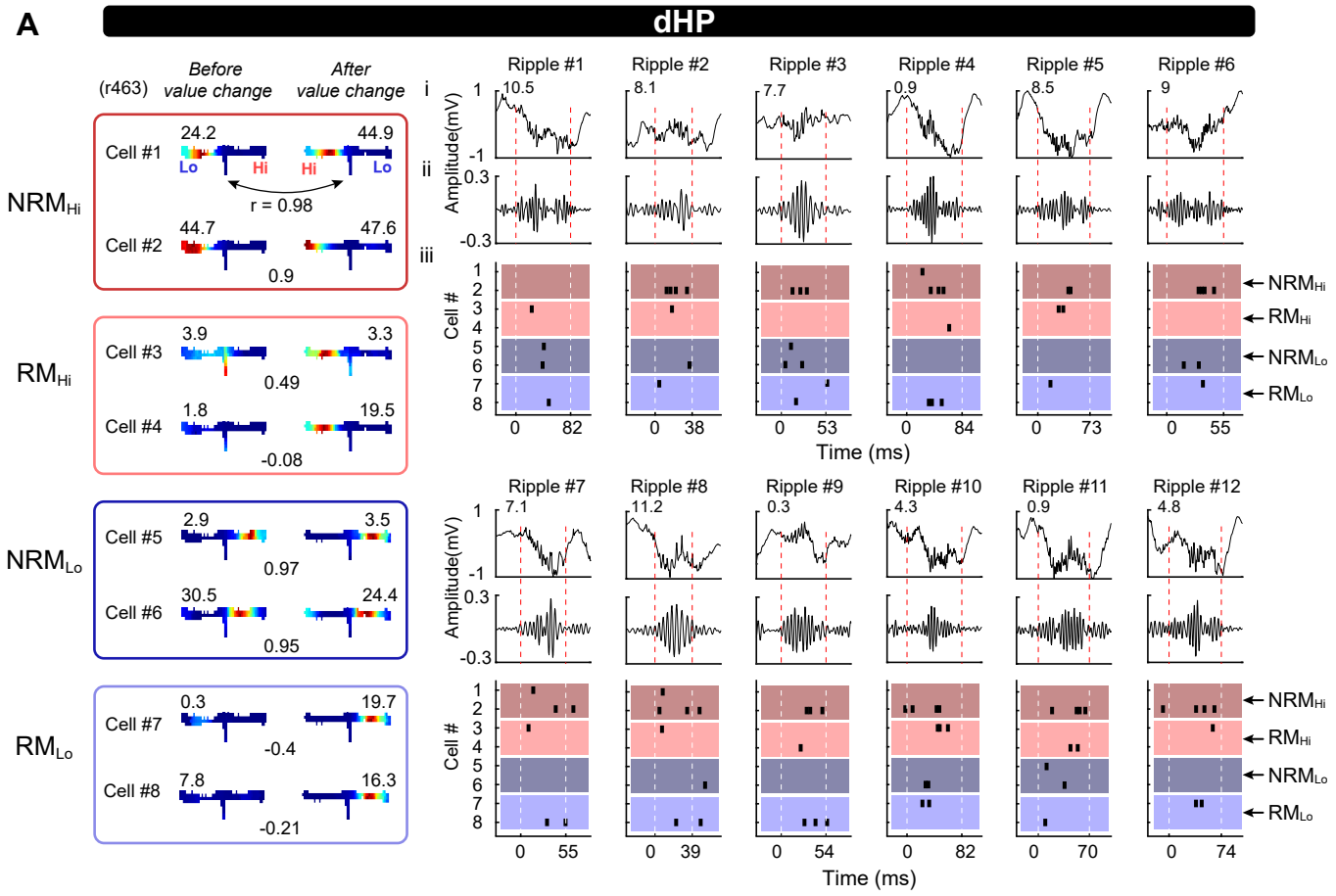
A
dHP
(r463)
Before value change
After value change
NRMHi
Cell #1
24.2
44.9
Lo
Hi
Hi
Lo
r = 0.98
Cell #2
44.7
47.6
0.9
RMHi
Cell #3
3.9
3.3
0.49
Cell #4
1.8
19.5
-0.08
NRMLo
Cell #5
2.9
3.5
0.97
Cell #6
30.5
24.4
0.95
RMLo
Cell #7
0.3
19.7
-0.4
Cell #8
7.8
16.3
-0.21
i
ii
iii
Ripple #1
10.5
Ripple #2
8.1
Ripple #3
7.7
Ripple #4
0.9
Ripple #5
8.5
Ripple #6
9
Amplitude(mV)
Cell #
Time (ms)
Ripple #7
7.1
Ripple #8
11.2
Ripple #9
0.3
Ripple #10
4.3
Ripple #11
0.9
Ripple #12
4.8
NRMHi
RMHi
NRMLo
RMLo

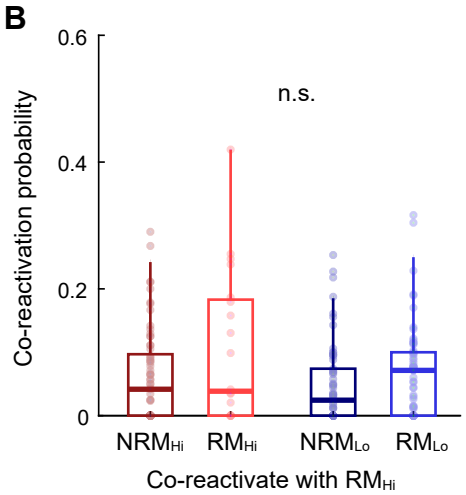
B
Co-reactivation probability
n.s.
NRMHi
RMHi
NRMLo
RMLo
Co-reactivate with RMHi

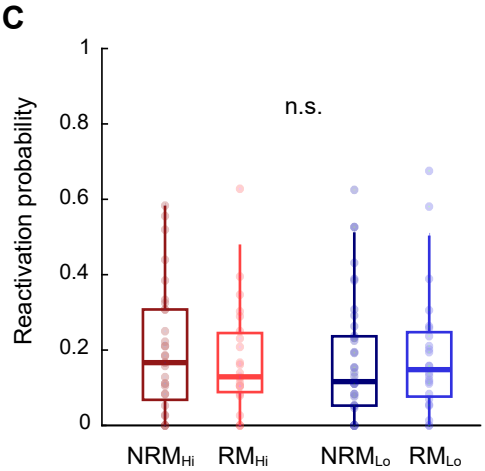
C
Reactivation probability
n.s.
NRMHi
RMHi
NRMLo
RMLo

Figure 6

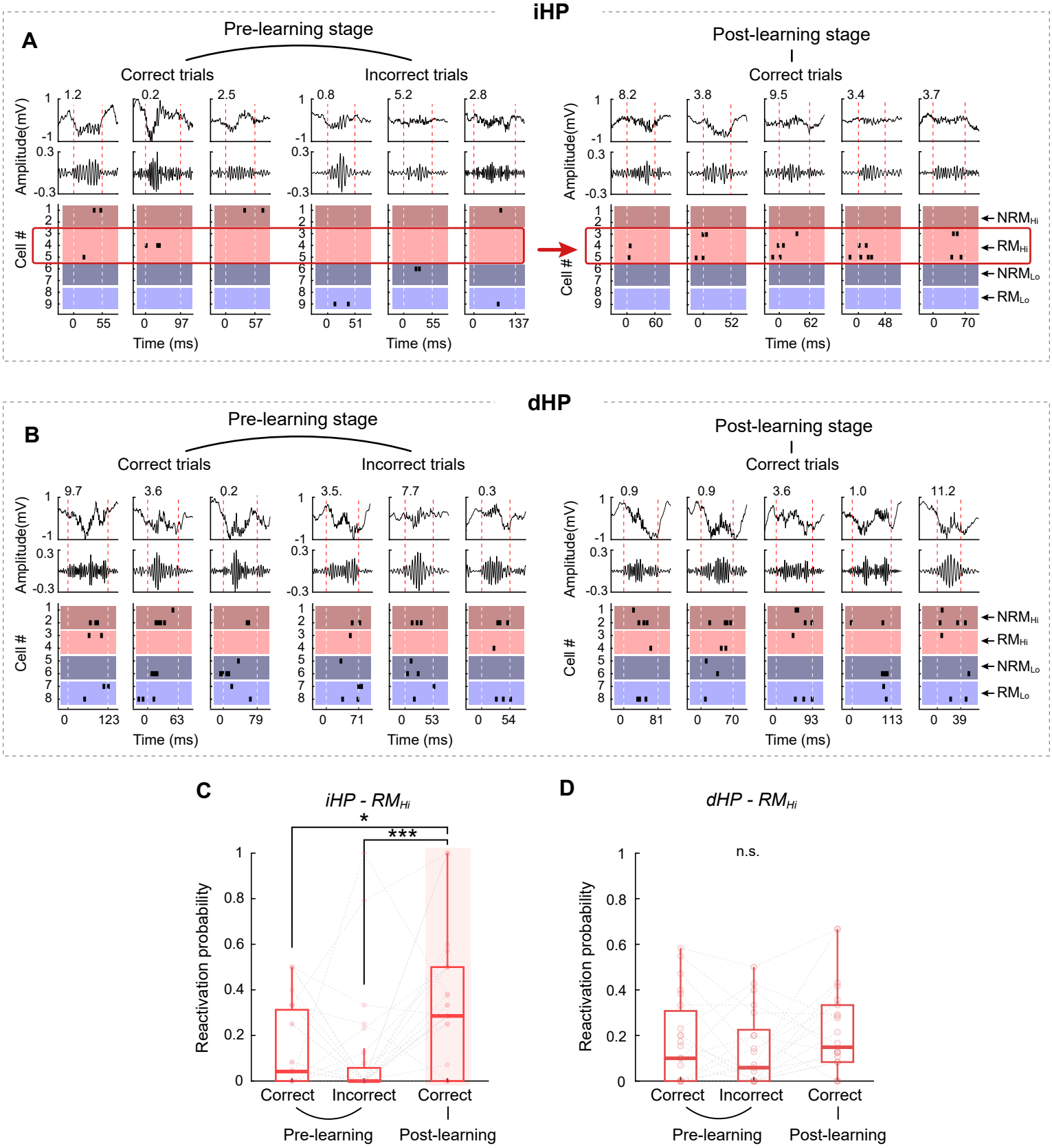
iHP
A
Pre-learning stage
Correct trials
Incorrect trials
Post-learning stage
Correct trials
Amplitude(mV)
Cell #
Time (ms)
NRM$_{Hi}$
RM$_{Hi}$
NRM$_{Lo}$
RM$_{Lo}$
dHP
B
Pre-learning stage
Correct trials
Incorrect trials
Post-learning stage
Correct trials
C
iHP - RM$_{Hi}$
Reactivation probability
Correct
Incorrect
Correct
Pre-learning
Post-learning
D
dHP - RM$_{Hi}$
n.s.
Reactivation probability
Correct
Incorrect
Correct
Pre-learning
Post-learning

Figure 7

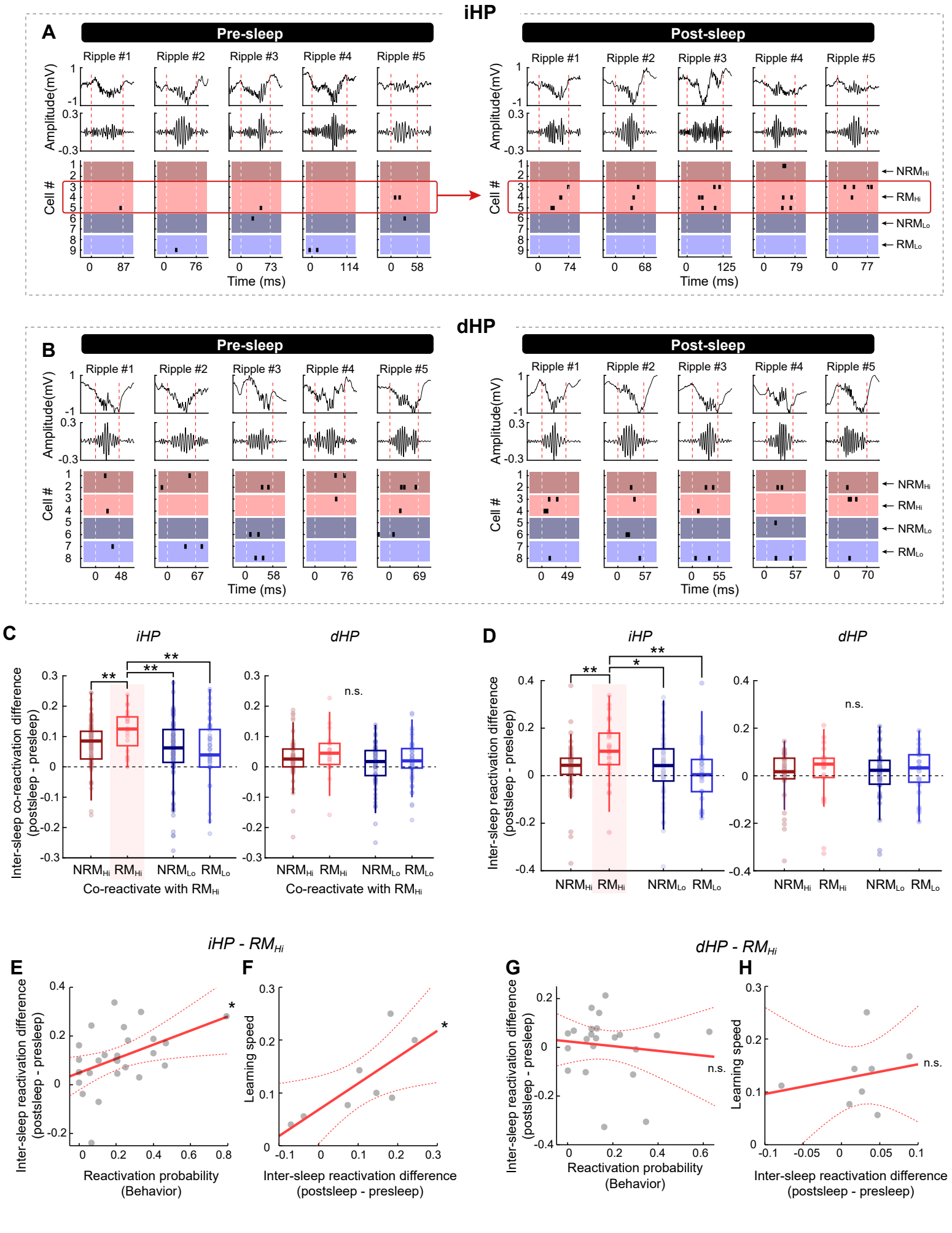
iHP
A
Pre-sleep
Post-sleep
Ripple #1
Ripple #2
Ripple #3
Ripple #4
Ripple #5
Amplitude(mV)
Cell #
Time (ms)
NRMHi
RMHi
NRMLo
RMLo
dHP
B
C
iHP
dHP
Inter-sleep co-reactivation difference (postsleep - presleep)
n.s.
Co-reactivate with RMHi
D
Inter-sleep reactivation difference (postsleep - presleep)
iHP - RMHi
dHP - RMHi
E
F
G
H
Reactivation probability (Behavior)
Learning speed
Inter-sleep reactivation difference (postsleep - presleep)

Figure 8

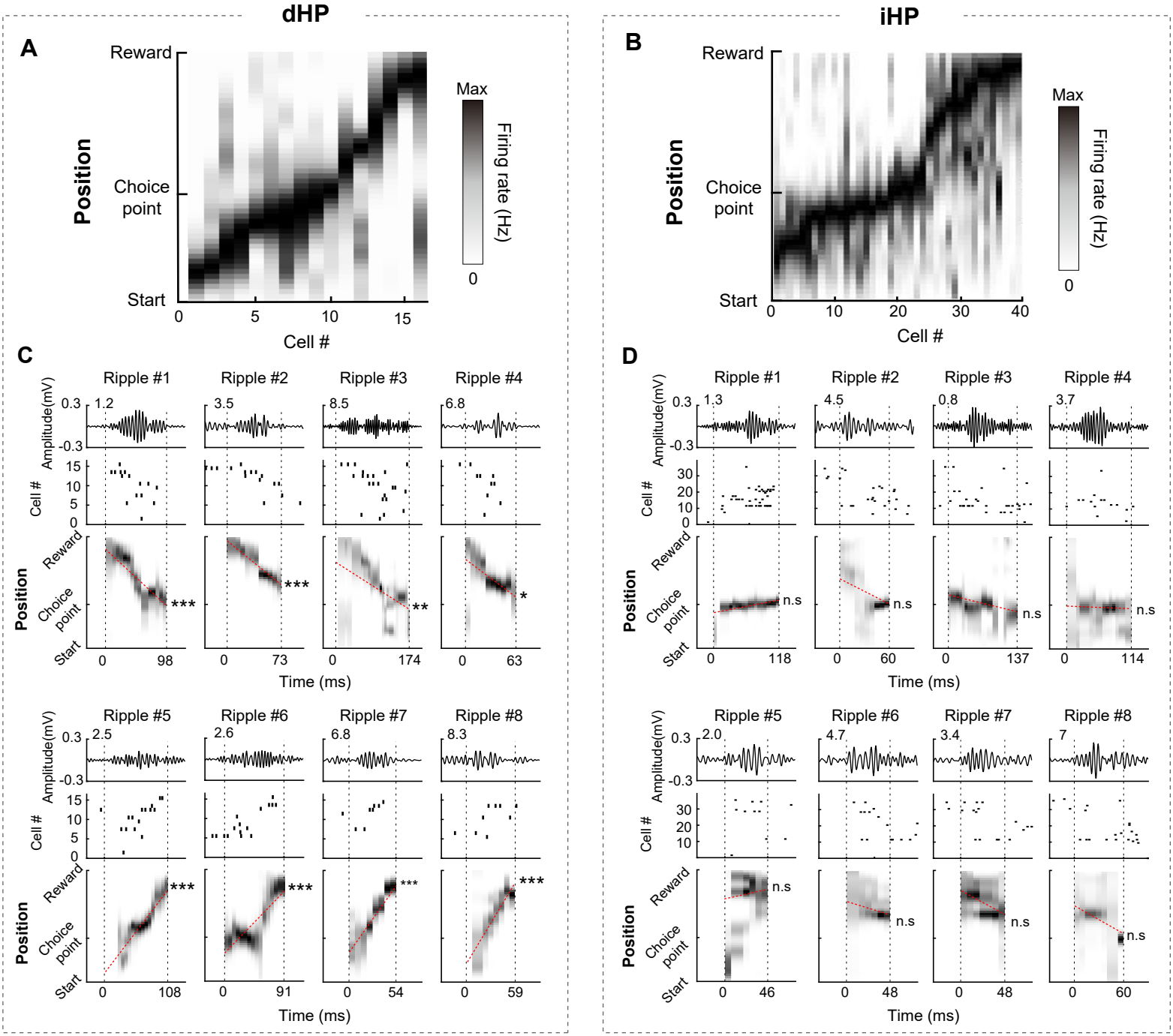
dHP
iHP
A
B
Reward
Choice point
Start
Position
Cell #
Max
Firing rate (Hz)
0
C
D
Ripple #1
Ripple #2
Ripple #3
Ripple #4
Ripple #5
Ripple #6
Ripple #7
Ripple #8
Amplitude(mV)
Time (ms)
n.s

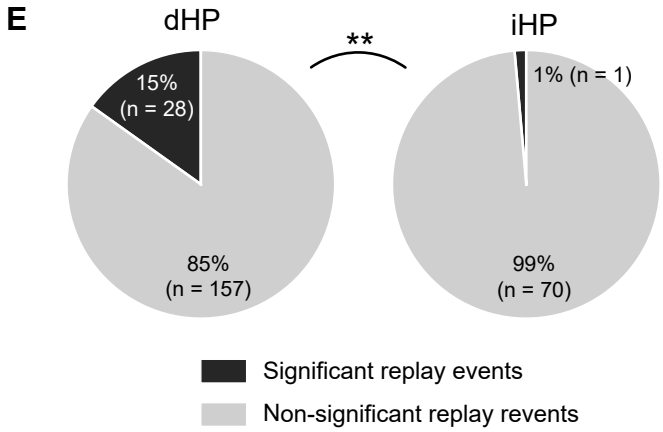
E
dHP
iHP
**
15% (n = 28)
85% (n = 157)
1% (n = 1)
99% (n = 70)
Significant replay events
Non-significant replay revents

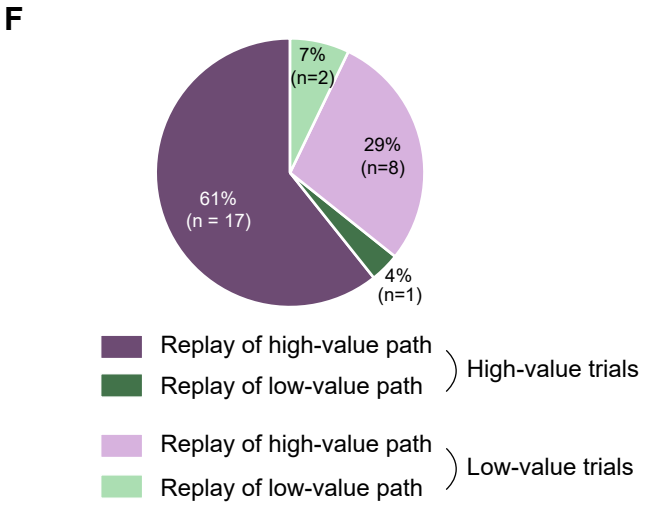
F
7% (n=2)
29% (n=8)
61% (n = 17)
4% (n=1)
Replay of high-value path
Replay of low-value path
High-value trials
Replay of high-value path
Replay of low-value path
Low-value trials